Accelerated, Sparsity-Aware Generalizations of Classical Algorithms for TomoPIV

Ioana Barbu, Cédric Herzet

11TH INTERNATIONAL SYMPOSIUM ON PARTICLE IMAGE VELOCIMETRY - PIV15
Santa Barbara, California, September 14-16, 2015

Accelerated, Sparsity-Aware Generalizations of Classical Algorithms for TomoPIV

Ioana Barbu[1] **and Cédric Herzet**[2]

[1]Irstea, UR TERE, F-35044, France
[2]Fluminance, INRIA Centre Rennes - Bretagne Atlantique, Rennes, France
[1]ioana.barbu@irstea.fr, [2]cedric.herzet@inria.fr

ABSTRACT

We set up a generalized optimization framework for the classical Row Action Methods, otherwise customarily employed in the TomoPIV community. This scheme allows us to bypass known caveats of the algebraic programs. The so-enhance methods enable *i)* handling explicit constraints on the signal; *ii)* accelerating the rates of convergence. Comparative numerical simulations reveal superior performance of the latter with no inflation of the complexity.

1. Introduction

Understanding the tridimensional (3D) motion of turbulent flows is one of the most challenging problems in experimental fluid dynamics. Since its inception, the "Particle Image Velocimetry" (PIV) [15] measurement technique has been the preferred *modus operandi* to tackle the turbulence from the experimental viewpoint. Recently, enhancements have been brought to the classical 2D scenario to enable 3D measurements. Within the so-called "Tomographic PIV (TomoPIV)" system, introduced by Elsinga *et al.* in [13], the 3D motion of a fluid is inferred from the observation of a multiview set of images captured at each time frame. A crucial step in this development is the volumetric reconstruction of the particles' distribution at each time frame. Pragmatical motivations have led TomoPIV scientists to take an interest in algorithms belonging to the class of "Row Action Methods" [9], which matched their expectations in terms of: *i)* data storage requirements; *ii)* computational time. This, on top of their implementation-friendly architecture and their ability to output satisfying solutions within a few iterations, has let the advances in the TomoPIV Volume Reconstruction Problem slowly come to a stall; moreover, other orthogonal solutions [5,20] – believed to be computationally more expensive – have missed their transition from numerical to experimental assessment. However, Row Action Methods suffer from a certain number of caveats: *i)* their rates of convergence are usually linear [12]; *ii)* they do not *explicitly* exploit the physical knowledge on the **sparse** and **noise-biased** nature of the TomoPIV signal.

In summary, there is a need for *i)* algorithms satisfying the storage and computational time requirements of the physical system; *ii)* procedures able to account for some physical *a priori* on the signal and robust to noise affecting the observations. We address this problem in the remainder of the paper. In particular, we show that procedures classically appointed for the TomoPIV volume reconstruction problem can be recast within a general optimization framework, **without any major change in their algorithmic architecture, nor the complexity thereof**, inducing, among other perks: *i)* higher convergence rates; *ii)* the possibility to apply powerful convex-optimization tools to solve the problem.

The paper is organized as follows. Section 2 formalizes the observation model used in our subsequent derivations. In Sections 3 and 4, we lay-out an intuitive setting to show the progress of classical algebraic procedures towards more evolved optimization schemes. Section 5 brings numerical validation that the more elaborate schemes encompassing SMARTs and SIRTs should be the preferred method for tackling the TomoPIV Volume Reconstruction problem, leading us naturally to an anticipated conclusion in Section 6.

2. Model and Related Works

In a nutshell, we aim at modelling the interaction between the illuminated passive tracers flowing in the measurement region and the planes of the cameras placed around the volume of interest.

The key element conditioning the design of a realistic model comes from the physical properties of the seeders. The latter dramatically influences the projection model. In fact, the projection of a small particle on an image impacts a small vicinity of pixels; the latter form "airy spots" on an image instead of dot-like projections. A good approximation of this phenomenon was given by *Champagnat et al.* in [10]. According to the said model, the image intensity y at a point $\mathbf{u} \in \mathbb{R}^2$ writes:

$$y(\mathbf{u}) = \sum_{p \in \{1,\dots,n_p\}} A(\mathbf{u} - P(\mathbf{k}_p)) x(\mathbf{k}_p), \tag{1}$$

where n_p counts the number of particles captured in the region of interest, $\mathbf{k}_p \in \mathbb{R}^3$ registers for the location of the p^{th} tracer in the volume

and functions $x : \mathbb{R}^3 \to \mathbb{R}_+$, $P : \mathbb{R}^3 \to \mathbb{R}^2$ and $A : \mathbb{R}^2 \to \mathbb{R}_+$ stand for the volume intensity, projection and the *Point Spread Function (PSF)* – which defines the formation of the airy spots –, respectively. We can easily arrive at a **discrete** analogue of (1), namely:

$$\mathbf{y} = \mathbf{A}\mathbf{x} + \text{noise}, \tag{2}$$

where $\mathbf{y} \in \mathbb{R}^m$ is a vector collecting the set of image pixels at points $\mathbf{u}$ belonging to the bidimensional image grids; $\mathbf{x} \in \mathbb{R}^n$ is a vector such that each element x_j is associated to a discretized particle position (*i.e.*, a voxel) in the visualized volume: $x_j = 0$ if and only if there is no particle at the corresponding location; finally, $\mathbf{A} \in \mathbb{R}^{m \times n}$ is the "projection matrix" which relates the collected images to some particle configuration $\mathbf{x}$. We refer the reader to [4, Chapter 2], for a detailed description of our model construction, which relies on an approximation of the PSF. The system (2) has a series of notable properties – *i)* $m \ll n$ and the inversion of (2) is seriously ill-posed; *ii)* the nonzero elements of $\mathbf{x}$ correspond to the energy scattered by the particles and are therefore nonnegative, *i.e.*, $\mathbf{x} \geq 0$; *iii)* the number of seeded particles is far less numerous than the number of voxels, *i.e.*, [1] $\|\mathbf{x}\|_0 \ll n$; *iv)* m and n are typically large (*e.g.*, $m \sim 10^6$, $n \sim 10^9$) – some of which may condition the choice of the method to invert the system.

3. Classical Algorithms

It is precisely the high dimensionality of the system (2) that motivated the TomoPIV community to resort to Row-Action Methods, interesting for their low computational and storage requirements. The latter encompass the well-known "Simultaneous Multiplicative Algebraic Reconstruction Technique (SMART)" [8] and the "Simultaneous Iterative Reconstruction Technique (SIRT)" [1, 11].

The SIRTs include, inter alia, known procedures such as "Cimmino" [11] or "SART" [1]. In its comprehensive form, a solution of (2) is sought as a fixed point of the following recursion

$$\mathbf{x}^{(k+1)} = \mathbf{x}^{(k)} + \alpha^{(k)} \mathbf{W}\mathbf{A}^T \Gamma(\mathbf{y} - \mathbf{A}\mathbf{x}^{(k)}), \tag{3}$$

where $\alpha^{(k)} > 0$ and $\mathbf{W}, \Gamma$ are some diagonal positive-definite matrices. In the sequel, we will use the simple notation $\mathbf{x}^{(k+1)} = \text{SIRT}(\mathbf{x}^{(k)})$ to denote the recursion defined by (3). Within the TomoPIV context, Cimmino and SART have been advocated in [18] and [17], respectively.

The most popular procedure for TomoPIV is the "Simultaneous Multiplicative Algebraic Reconstruction Technique" (SMART) [8]. The iterates can be expressed as

$$x_j^{(k+1)} = x_j^{(k)} \prod_{i=1}^{m} \left(\frac{y_i}{\mathbf{a}_i^T \mathbf{x}^{(k)}} \right)^{\gamma a_{ij}} \quad \forall\, j, \tag{4}$$

where $\gamma > 0$ and $\mathbf{a}_i \in \mathbb{R}^n$ is the ith row of $\mathbf{A}$. Henceforth, we will use the simple notation $\mathbf{x}^{(k+1)} = \text{SMART}(\mathbf{x}^{(k)})$ to denote the recursion defined in (4). SMART was introduced into the TomoPIV setting in [2], before being broadly relayed by most contributors.

Although conceptually interesting, SIRT and SMART do not allow to account for other known trademarks of the $\mathbf{x}$ – more specifically, its sparsity – and they can have a very low speed of convergence, especially for highly-seeded fluids.

4. Towards an Optimization Framework

In this section, we expose our proposed methodology. We start by introducing some useful notations. Then, we show that by simply modifying classical procedures with regard to an optimization framework we can circumvent known shortcomings of the former.

4.1 Notations

We define the indicator function $\mathbb{I}_{\mathcal{X}}(\mathbf{x})$ of a set $\mathcal{X}$ as

$$\mathbb{I}_{\mathcal{X}}(\mathbf{x}) = \begin{cases} 0 & \text{if } \mathbf{x} \in \mathcal{X}, \\ +\infty & \text{otherwise.} \end{cases}$$

The proximal operator of a convex proper function $\mathrm{f} : \mathbb{R}^n \to \mathbb{R} \cup \infty$ is defined as

$$\text{prox}_{\mathrm{f}}(\mathbf{v}) = \underset{\mathbf{x} \in \mathcal{X}}{\arg\min}\, \mathrm{f}(\mathbf{x}) + \frac{1}{2}\|\mathbf{x} - \mathbf{v}\|_2^2.$$

[1] Here the notation $\|\mathbf{x}\|_0$ refers to the "ℓ_0-norm" which returns the number of nonzero elements in its argument.

4.2 SIRT and SMART as Particular Cases of Optimization Programs

We first notice that SIRT can be interpreted as a proximal gradient method (PGM) [16], which is an algorithmic variant of the well-know gradient projected method. In fact, the SIRT iteration depicted by Equation (3) corresponds to the PGM step when the latter procedure is applied to problem:

$$\min_{\mathbf{x}} \frac{1}{2}\|\mathbf{y}-\mathbf{A}\mathbf{x}\|_2^2 + \lambda \mathrm{r}(\mathbf{x}), \tag{5}$$

provided that $\mathbf{W}=\mathbf{I}$, $\Gamma=\mathbf{I}$ and $\mathrm{r}(\mathbf{x})$ is constant function, while $\lambda>0$ is some tuning parameter.

We can enforce the sparsity and the nonnegativity of the sought solution by an appropriate choice of $\mathrm{r}(\mathbf{x})$. For example, let $\mathrm{r}(\mathbf{x}) = \lambda\|\mathbf{x}\|_1 + \mathbb{I}_{\mathbb{R}^n_+}(\mathbf{x})$, the PGM recursion reads as

$$\mathbf{x}^{(k+1)} = \mathrm{prox}_{\lambda\|\mathbf{x}\|_1+\mathbb{I}_{\mathbb{R}^n_+}}(\mathrm{SIRT}(\mathbf{x}^{(k)})), \tag{6}$$

where the proximal operator $\mathrm{prox}_{\lambda\|\mathbf{x}\|_1+\mathbb{I}_{\mathbb{R}^n_+}}(\cdot)$ takes the simple form:

$$\left(\mathrm{prox}_{\lambda\|\mathbf{x}\|_1+\mathbb{I}_{\mathbb{R}^n_+}}(\mathbf{v})\right)_i = \begin{cases} v_i-\lambda & \text{if } v_i \geq \lambda \\ 0 & \text{otherwise.} \end{cases} \tag{7}$$

Plugging Equation (7) into Equation (6) translates to the projection on the positive orthant of the *soft thresholded* current estimate. Simply put, enforcing the positivity and the sparsity of the solution comes down to computing a SIRT iteration, followed by a simple thresholding operation of the solution (which induces no inflation of the complexity cost).

In an equivalent manner, we recognize that SMART can be interpreted as a nonlinear projected gradient (NPG) algorithm [6, 19] which is also a variant of the gradient projected method – applied to problem:

$$\min_{\mathbf{x}\in\mathcal{X}} \mathrm{KL}(\mathbf{y},\mathbf{A}\mathbf{x}), \tag{8}$$

with $\mathcal{X}=\mathbb{R}^n_+$ and where $\mathrm{KL}(\cdot,\cdot)$ denotes the Kullback-Leibler distance between two nonnegative vectors.

The sparsity of the sought solution can then simply be imposed by adding the additional constraint "$\|\mathbf{x}\|_1 \leq \tau$" to problem (8). This is equivalent to contraining the optimization set to be of the form $\mathcal{X}=\{\mathbf{x}\in\mathbb{R}^n_+ | \mathbf{1}^T\mathbf{x}\leq\tau\}$. With this particular choice for $\mathcal{X}$, it can be shown that the NPG iterates still obey a closed-form recursion:

$$\mathbf{x}^{(k+1)} = \begin{cases} \tilde{\mathbf{x}}^{(k+1)} & \text{if } \mathbf{1}^T\tilde{\mathbf{x}}^{(k+1)} \leq \tau \\ \tau\frac{\tilde{\mathbf{x}}^{(k+1)}}{\mathbf{1}^T\tilde{\mathbf{x}}^{(k+1)}} & \text{otherwise,} \end{cases} \tag{9}$$

where $\tilde{\mathbf{x}}^{(k+1)} = \mathrm{SMART}(\mathbf{x}^{(k)})$. Altogether, the "sparsity-aware" SMART iteration is updated conditionally: following the ubiquitous Equation (4), if the current estimate is sparse enough and by the SMART solution normalized by the ℓ_1-norm of the estimate, otherwise. Seemingly, no significant complexity cost is induced by this update.

The identification of SIRT and SMART as instances of PGM and NPG algorithms, respectively, allows us to propose an accelerated version of this type of procedures. In order to do so, we adopt the strategies proposed in [7] (respectively [3, Section 5]) which achieves a rate of decrease of the cost function scaling as $O(k^{-2})$ (versus $O(k^{-1})$ for the standard procedures) by applying the PGM update $\mathbf{x}^{(k+1)} = \mathrm{SIRT}(\mathbf{z}^{(k+1)})$ (respectively, the NPG update $\tilde{\mathbf{x}}^{(k+1)} = \mathrm{SMART}(\mathbf{z}^{(k+1)})$) to a proper interpolation point

$$\mathbf{z}^{(k+1)} = \mathbf{x}^{(k)} + \zeta^{(k)}(\mathbf{x}^{(k)} - \mathbf{x}^{(k-1)}), \tag{10}$$

with $\zeta^{(k)} \in [0,1]$. We notice that the operation (10) induces no inflation of the complexity order.

5. Numerical Validation

We carry out a comparative numerical assessment of the classical methods *versus* their enhanced counterparts. Nomenclature-wise, sparsity-aware variants of SIRT and SMART will respectively append "ℓ_1" to their label (see equations (6) and (9), respectively). We will prefix the accelerated versions of the classical algorithms (and of their sparsity-enhanced companions) by "A-" in our figure legend.

We simulate a medium-scale perturbed setting (*i.e.*, $m=6724$, $n=99944$), where y_i is affected by a Gaussian noise of zero mean and standard deviation equal to $0.1y_i$. The results are averaged on 10 experiments and we allow for 100 iterations. The relaxation parameter γ (see Equation (4)) is initially chosen as $0.1, 0.05, 0.4$ and 0.8 for SMART, A-SMART, SMARTℓ_1 and A-SMARTℓ_1, respectively, while $\lambda=0.01$ (see Equation (5)). The so-chosen initial values of λ is then iteratively adapted following the Armijo rule. We set $\tau=\|\mathbf{x}\|_0$ (where $\mathbf{x}$ is the ground truth whose non-zero coefficients equal 0) – see Equation (9). As suggested in [16], we update $\zeta^{(k)}=\frac{k}{k+3}$; for specifics of this action relate to Equation (10).

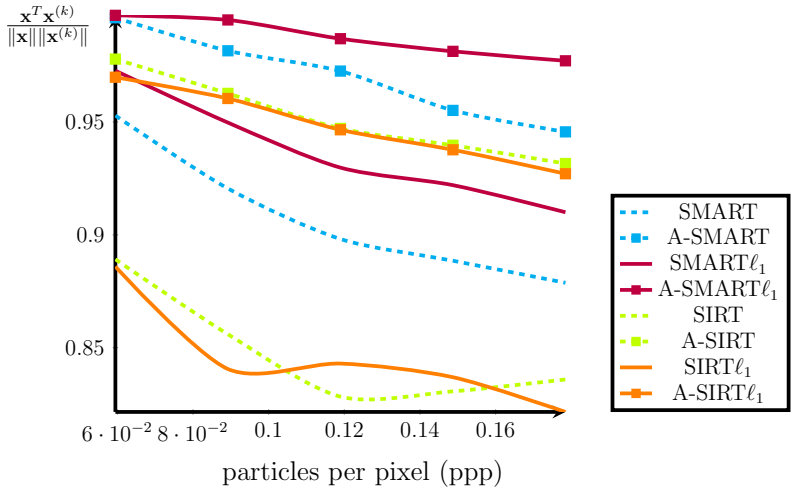

Figure 1: Numerical assessment of the reconstruction quality of $\mathbf{x}^{(100)}$ in terms of the normalized correlation against the "particles per pixel (ppp)" ratio.

Figure 1 illustrates the performance achieved by the proposed methods. The abscissa represents the sparsity level of the sought vector $\mathbf{x}$, expressed in terms of the "particles per pixel (ppp) ratio" (see [14]), and the ordinate is the normalized correlation $\frac{\mathbf{x}^T\mathbf{x}^{(k)}}{\|\mathbf{x}\|\|\mathbf{x}^{(k)}\|}$, a figure of merit commonly used in the Tomographic PIV community. We notice in particular that *i)* standard algorithms are outperformed by their accelerated versions, despite solving the same convex problem – this is due to the higher convergence rates of the latter; *ii)* generally, the unregularized algorithms are outperformed by their "sparsity-aware" counterparts – this is achieved by accounting for an additional information on the signal when solving the inverse TomoPIV problem.

6. Conclusion

This paper campaigns for the understanding of some classical Row Action Methods from the optimization viewpoint. The advantage of tackling the TomoPIV problem from this angle is twofold. First, the algorithmic structure barely suffers any change as the proposed scheme yields closed-form updates which do not affect the complexity cost, nor the parallelizable architecture of SMART. Second, the newly-found mathematical properties allow for a remarkable flexibility to obtain accelerated, sparsity-aware enhancements and merit further extensive study.

References

[1] A.H. Andersen and A.C. Kak. Simultaneous Algebraic Reconstruction Technique (SART): a superior implementation of the ART algorithm. *Ultasonic Imaging*, 6, 1984.

[2] C. H. Atkinson and J. Soria. An efficient simultaneous reconstruction technique for tomographic particle image velocimetry. *Exp. Fluids*, 47(4-5), 2009.

[3] A. Auslender and M. Teboulle. Interior gradient and proximal methods for convex and conic optimization. *SIAM J. Sci. Comput.*, 16(3), 2006.

[4] I. Barbu. *Tridimensional Estimation of Turbulent Fluid Velocity*. PhD thesis, Université Rennes 1, 2014.

[5] I. Barbu, C. Herzet, and E. Mémin. Sparse models and pursuit algorithms for PIV tomography. In *FVR*, 2011.

[6] A. Beck and M. Teboulle. Mirror descent and nonlinear projected subgradient methods for convex optimization. *Oper. Res. Lett.*, 31(3), 2003.

[7] A. Beck and M. Teboulle. A Fast Iterative Shrinkage-Thresholding Algorithm for Linear Inverse Problems. *SIAM J. Imaging Sci.*, 31(3), 2009.

[8] C.L. Byrne. Iterative Image Reconstruction Algorithms Based on Cross-Entropy Minimization. *IEEE Trans. Image Process.*, 2(1), 1993.

[9] Y. A. Censor and S. A. Zenios. *Parallel Optimization: Theory, Algorithms and Applications*. Oxford University Press, 1997.

[10] F. Champagnat, P. Cornic, A. Cheminet, B. Leclaire, and G. Besnerais. Tomographic PIV: particles vs blobs. In *PIV*, 2013.

[11] G. Cimmino. Calcolo approsimato per le soluzioni dei sistemi di equazioni lineari. *La Ric. Sci.*, 14(2), 1938.

[12] T. Elfving. On Some Methods for Entropy Maximization and Matrix Scaling. *Linear Algebra Appl.*, 34(12), 1980.

[13] G. Elsinga, F. Scarano, B. Wieneke, and B. van Oudheusden. Tomographic particle image velocimetry. *Exp. Fluids*, 41(6), 2006.

[14] G. E. Elsinga. *Tomographic particle image velocimetry*. PhD thesis, Technische Universiteit Delft, 2008.

[15] R. Meynart. Digital image processing for speckle flow velocimetry. *Rev. Sci. Instrum.*, 29(35), 1982.

[16] N. Parikh and S.P. Boyd. Proximal Algorithms. *Found. Trends Optim.*, 2013.

[17] S. Petra, C. Popa, and C. Schnörr. Enhancing Sparsity by Constraining Strategies: Constrained SIRT versus Spectral Projected Gradient Methods. In *VMM*, 2008.

[18] S. Petra, C. Popa, and C. Schnörr. Extended and Constrained Cimmino-type Algorithms with Applications in Tomographic Image Reconstruciton. *Int. J. Comput. Math.*, 2010.

[19] S. Petra, C. Schnörr, F. Becker, and F. Lenzen. B-SMART: Bregman-Based First-Order Algorithms for Non-negative Compressed Sensing Problems. In *SSVM*, 2013.

[20] S. Petra, A. Schröder, B. Wieneke, and C. Schnörr. On Sparsity Maximization in Tomographic Particle Image Reconstruction. In *Proceedings of the 30th DAGM Symposium on Pattern Recognition*, 2008.